

Critical Micelle Concentration of Micelles with Different Geometries in Diblock Copolymer/Homopolymer Blends

Jiajia Zhou* and An-Chang Shi†

Department of Physics & Astronomy, McMaster University

Hamilton, Ontario, Canada L8S 4M1

(Dated: August 14, 2011)

Abstract

It is well-known that A-B diblock copolymers in selective solvents or A-homopolymers can form micelles of different shapes. The critical micelle concentration (CMC) of three basic micelle shapes (lamellar, cylindrical and spherical) are calculated using the self-consistent field theory formulated in the grand canonical ensemble. For a given set of molecular parameters, the stable micelle morphology is determined by a comparison of the CMC. The results confirm that micelles undergo a sequence of shape transitions, lamellar \rightarrow cylindrical \rightarrow spherical, when the A-block of the diblock copolymer becomes longer. The results also reveal details about the micelle structure, such as the core radius and corona thickness. This information can be used to understand the effect of homopolymer molecular weight and monomer-monomer interaction on the micelle morphologies.

*present address: Institut für Physik, Johannes Gutenberg-Universität, Staudingerweg 7, D-55099 Mainz, Germany. E-mail: zhou@uni-mainz.de

†E-mail: shi@mcmaster.ca

I. INTRODUCTION

Block copolymers are polymers consist of two or more different types of polymeric components, or blocks, covalently linked together. The simplest block copolymer is the AB diblock copolymer, where two distinct blocks, A and B, are linked end-to-end by a covalent bond [1]. The physical property of diblock copolymers is dictated by the combined effects of two competing interactions, i.e., the repulsion between, and the connectivity of, the two different blocks. The simplicity of diblock copolymer architecture makes it an ideal model system to study self-assembly of amphiphilic molecules. One intriguing example of the self-assembly is the micelle formation of diblock copolymers blended with homopolymers which are chemically identical to one of the blocks (the AB/A blends) [2]. The repulsive interaction between different monomers leads to the formation of aggregates while the covalent bonds between the incompatible blocks prevent a macrophase separation, leading to the formation of micelles of different shapes. Similar phenomenon occurs for other amphiphilic molecules, such as the segregation of surfactants in water and the bilayer formation of lipids. A comprehensive understanding of the micellization in diblock copolymer/homopolymer blends is important from the fundamental polymer physics point of view. Furthermore, such an understanding may also provide insight to the physical properties of more complicated biological systems.

The micelle formation can be understand by considering the process of adding AB diblock copolymers to a melt of A-homopolymers. At low block copolymer concentration, diblock copolymers stay as isolated chains in the homopolymer matrix. As the copolymers concentration is increased, the B-blocks of the AB diblock copolymers tend to cluster together to form micellar aggregates. The formation of micelles leads to a local separation of the A and B blocks, leaving an AB interface between the B and A domains, thus reducing the unfavorable contact between B-blocks and A-homopolymers since the A-blocks acts like a shield. The copolymer concentration at which micelles start to emerge is termed the critical micelle concentration (CMC) [3]. The most common micelles have a spherical shape, consisting of a core of B-blocks surrounded by a corona of A-blocks. Other micelle morphologies, such as cylindrical or lamellar, have been observed in experiments [4]. The preferred micelle shape is determined by several parameters, including the copolymer concentration, the diblock asymmetry, the copolymer/homopolymer length ratio, and the monomer-monomer interaction. These micelles have a characteristic size which is larger than those of a single molecule,

but they do not become macroscopic objects. Compared to micelles formed by surfactants with low molecular weights, the block copolymer micelles are more stable, and the micelle size can be adjusted by varying the molecular weight. The stability and the adjustability make copolymer micelles a suitable candidate for potential applications, particularly for drug delivery [5].

Micelle formation in diblock copolymer/homopolymer blends has been studied extensively using analytic methods and simulations. Some systematic experimental investigations have also been carried out [4]. On the theory front, several authors employed the scaling argument to derive an analytic form of the total free energy for the micelle state [6–13]. Generically, the free energy of a micelle contains contributions from the core, the corona and the interface. Each contribution can be obtained in terms of several independent variables, such as the number of copolymers per micelle, the core radius, the corona thickness. The free energy of the micelle state then can be minimized, leading to an equilibrium micelle size. The comparison of the micelle free energy with the homogeneous state is then made to determine the stability of the micelle state. The analytic nature of these methods allows for exploring the rich phase behaviors of micelle system as a function of molecular architecture, composition, and monomer incompatibility. The complexity and validity of the approach depends on the blend properties. For example, long homopolymers are difficult to penetrate into the corona, thus micelles can be viewed to consist entirely of copolymer chains. This simplifies the model considerably. Using this approximation, Leibler [6] studied spherical micelles, and later Shull *et al.* [7, 8] extended the model to include cylindrical and lamellar micelles. When the homopolymers have a length compatible to that of the copolymers, they can swell the corona of the micelles. Leibler *et al.* [9] considered the formation of spherical micelles in this case. Later the theory was extended by Whitmore and Noolandi [10] to allow the swelling of the micelle core. The transition between different morphologies was first studied by Mayes *et al.* [12]. They employed a refined free energy model and focused on the sphere to cylinder transition. Most of these models assumed that micelles are monodisperse; the effect of polydispersity has been studied by Kao *et al.* [13]. The prediction and the applicable region of different analytical approaches have been reviewed by Milchev *et al.*[14].

The scaling approach considers only the dominant contributions to the total free energy, so an analytical expression can be obtained. The polymer conformations are usually simplified

as strongly stretched lines in the scaling theory. In order to make a quantitative comparison with experiments, we need to consider all contributions and numerical simulations are usually required. There are a number of simulation studies of the micelle formation in diblock copolymer/homopolymer blends and other similar systems. Mackie *et al.* [15] and Guerin *et al.* [16] employed the single-chain mean-field theory to examine micelle formations. Smit *et al.* [17] used molecular dynamics simulation to study surfactant self-assembling in the water. Monte-Carlo simulations have also been implemented by several authors [14, 18–23]. In particular, Pepin and Whitmore [19] compared the scaling relation predicted by the analytic method to their Monte-Carlo simulation results, and Termonia [22] studied the sphere-to-cylinder transition of AB diblock copolymer micelles in a selective solvent. Most simulations treated solvents (or A-homopolymers) explicitly, and it becomes computationally challenging to simulate long chains and large system. Computational improvement has been made by Sheng *et al.* [24] using dissipative particle dynamics.

All these previous simulations are particle-based, in which each polymer is modeled as a long chain consisted of connected beads. A simulation on a large system with many long chains is, therefore, computationally expensive. As such, the particle-based simulations are mostly done in systems involving solvents of low molecular weight. For solvents consisting of long homopolymer chains, field-based methods are the natural choice. Self-consistent field theory (SCFT) is a powerful theoretical method to model polymer systems, and its molecular-level accuracy can provide detailed information about the micelle structure [8, 23, 25–30]. Early attempts [8, 25, 26] of SCFT study of micelles used a lattice-based numerical calculation. Duque [27] employed the theory with an additional constraint that permits the examination of intermediate structures. Chang *et al.* [28] used a pressure difference to stabilize the micelle. Very recently Greenall *et al.* [29, 30] studied the micelle formation and shape transition by a method of varying the size of the simulation box. These authors designed their model such that it corresponds to the experimental systems of Kinning *et al.* [4], and made detailed comparison with the experimental results. Furthermore, Cavallo, Müller and Binder [23] also employed SCFT calculations in the (semi-)grandcanonical ensemble, and compared their results with Monte Carlo simulations. These studies have greatly enriched our understanding of the micelle formation. However, there still lacks a thorough investigation of the shape transition by changing various parameters.

In this paper, we use self-consistent field theory to model an isolated micelle in blends of

AB diblock copolymers and A homopolymers. We consider three different micelle morphologies: lamellar, cylindrical and spherical. We focus on the shape transition of the micelle and the effects of the diblock asymmetry, the homopolymer length and the interaction parameter.

II. SELF-CONSISTENT FIELD THEORY

The self-consistent field theory (SCFT) of polymeric systems has been described in detail by many authors [31–35]. In this section, we introduce the notations and summarize the important results for a binary blend of AB/A.

The blend is composed of AB diblock copolymers with a chain length N , and A-homopolymers with a chain length κN . The polymers are contained in a volume of V . The block copolymer is composed of a fraction f_A of the A-monomers, and a fraction $f_B (= 1 - f_A)$ of the B-monomers. We assume that the blend is incompressible and all the monomers have the same volume ρ_0^{-1} and statistical length a . The monomer-monomer interaction is characterized by the standard Flory-Huggins parameter χ . We formulate our theory in the grand-canonical ensemble. The incompressibility permits the choice of setting the chemical potential for homopolymers to be zero, and the controlling parameter is the copolymer chemical potential μ_c , or equivalently, the activity $z_c \equiv \exp(\mu_c)/\kappa$.

In the framework of self-consistent field theory, the system consisting many interacting chains is replaced by a system composed of many ideal Gaussian chains in an averaged effective mean-field potential. The potential is in turn depends on the conformation of the chains. The grand partition function of the system can be written as a functional integration over the densities $\{\phi\}$ and their conjugate fields $\{\omega\}$,

$$Z = \int \mathcal{D}\{\phi\} \mathcal{D}\{\omega\} \exp(-G/k_B T), \quad (1)$$

where the grand free energy G can be written in the form

$$\begin{aligned} \frac{NG}{k_B T \rho_0} = & \frac{1}{V} \int d\mathbf{r} [\chi N \phi_A(\mathbf{r}) \phi_B(\mathbf{r})] \\ & - \frac{1}{V} \int d\mathbf{r} [\omega_A(\mathbf{r}) \phi_A(\mathbf{r}) + \omega_B(\mathbf{r}) \phi_B(\mathbf{r})] \\ & - \frac{1}{V} \int d\mathbf{r} \xi(\mathbf{r}) [1 - \phi_A(\mathbf{r}) - \phi_B(\mathbf{r})] \\ & - z_c Q_c - Q_h. \end{aligned} \quad (2)$$

The first term is the intermolecular interaction energy, which is proportional to χN ; the second and third term present the coupling between the densities and their conjugate fields; the fourth term introduces a Lagrange multiplier $\xi(\mathbf{r})$ to enforce the incompressibility; and the last two terms are the configuration entropy, related to the single-chain partition functions for two polymers, Q_c and Q_h . For the copolymer, the partition function has a form $Q_c = \int d\mathbf{r} q_c(\mathbf{r}, 1)$, where $q_c(\mathbf{r}, s)$ is an end-integrated propagator, and s is a parameter runs from 0 to 1 along the length of the copolymer. The propagator satisfies the modified diffusion equation

$$\frac{\partial q_c}{\partial s} = \frac{1}{6} N a^2 \nabla^2 q_c - \omega_\alpha q_c, \quad (3)$$

where $\alpha = A$ if $0 < s < f_A$ and $\alpha = B$ if $f_A < s < 1$. The initial condition is $q_c(\mathbf{r}, 0) = 1$. Since the copolymer has two distinct ends, another end-integrated propagator $q_c^+(\mathbf{r}, s)$ is introduced. It satisfies Eqn. (3) with the right-hand side multiplied by -1 , and initial condition $q_c^+(\mathbf{r}, 1) = 1$. For the homopolymer, one propagator $q_h(\mathbf{r}, s)$ is sufficient, and the single-chain partition function has a form $Q_h = \int d\mathbf{r} q_h(\mathbf{r}, 1)$.

Because exact evaluation of the partition function is in general difficult, various approximations have been developed to evaluate the partition function. The most fruitful method is the mean field approximation, which amounts to evaluate the function integral using a saddle-point technique. Technically the saddle-point approximation is obtained by demanding that the function derivatives of the grand free energy expression (2) to be zero,

$$\frac{\delta G}{\delta \phi_\alpha} = \frac{\delta G}{\delta \omega_\alpha} = \frac{\delta G}{\delta \xi} = 0. \quad (4)$$

These conditions lead to the following mean-field equations,

$$\begin{aligned} \phi_A(\mathbf{r}) &= \int_0^\kappa ds q_h(\mathbf{r}, s) q_h(\mathbf{r}, \kappa - s) \\ &\quad + z_c \int_0^{f_A} ds q_c(\mathbf{r}, s) q_c^+(\mathbf{r}, s) \end{aligned} \quad (5)$$

$$\phi_B(\mathbf{r}) = z_c \int_{f_A}^1 ds q_c(\mathbf{r}, s) q_c^+(\mathbf{r}, s), \quad (6)$$

$$\omega_A(\mathbf{r}) = \chi N \phi_B(\mathbf{r}) + \xi(\mathbf{r}), \quad (7)$$

$$\omega_B(\mathbf{r}) = \chi N \phi_A(\mathbf{r}) + \xi(\mathbf{r}), \quad (8)$$

$$1 = \phi_A(\mathbf{r}) + \phi_B(\mathbf{r}). \quad (9)$$

These equations can be solved using iteration method.

The SCFT equations can be easily implemented in planar, cylindrical and spherical geometry, with the purpose to model micelles of different morphologies. This simplifies the problem to be one dimensional, and the modified diffusion equations can be solved in real space using the Crank-Nicholson method [36]. In our study, it is essential to calculate the free energy accurately. We have used a fine grid, with 200 space points per $\sqrt{N}a$ and 2000 points along the chain. It is also important to set the appropriate starting condition for the iteration, and we choose to set the micelle initially with a tanh density profile. In addition, we have run the calculations with different initial configurations to ensure that the converged solution is independent of the starting radius.

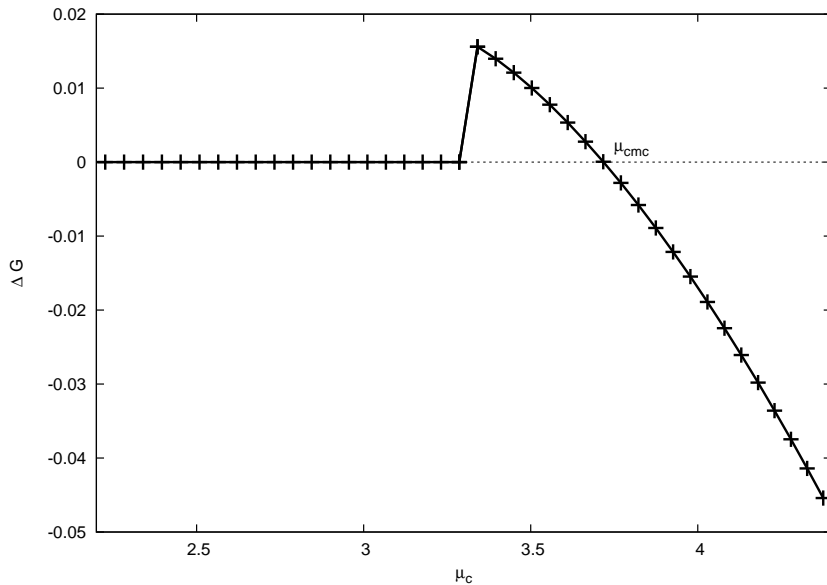


FIG. 1: Free energy difference ΔG between a cylindrical micelle and the homogeneous phase, plotted as a function of copolymer chemical potential μ_c . The blends have the parameters $f_A = 0.60$, $\kappa = 1.0$ and $\chi N = 20$.

The stability of the micelle is determined by comparing its free energy with the free energy of the homogeneous phase. Fig. 1 shows ΔG , the free energy difference between a cylindrical micelle and the homogeneous phase, plotted as a function of the copolymer chemical potential μ_c . The parameters of the blends used in this particular calculation are $f_A = 0.60$, $\kappa = 1.0$ and $\chi N = 20$. For large values of μ_c , corresponding to high copolymer concentration, the free energy difference ΔG is negative, indicating that the micelles are more stable than the homogeneous state. When μ_c approaches a critical value, μ_{cmc} , from

above, ΔG increases, and becomes positive when μ_c is smaller than μ_{cmc} . In what follows we define the CMC as the copolymer concentration at which the excess free energy changes sign. By using this definition, we have neglected the micelle-micelle interactions and the translational entropy of the micelles. Since we are mostly interested in the blends of small copolymer concentrations, the density of micelles is small so the micelle-micelle interaction contributions is negligible. On the other hand, the translation entropy of the micelles can be estimated by considering the volume occupied by the micelles [29, 30]. Because we are focusing on the shape transition of the micelles, the translation entropy contribution, which is insensitive to the micelle shapes, can be ignored. Once the μ_{cmc} is found, the critical micelle concentration can be calculated from the bulk relation,

$$\frac{\mu_c}{\kappa} = \frac{\ln \phi_c}{\kappa} - \ln(1 - \phi_c) + f_B \chi N (1 - 2f_B \phi_c). \quad (10)$$

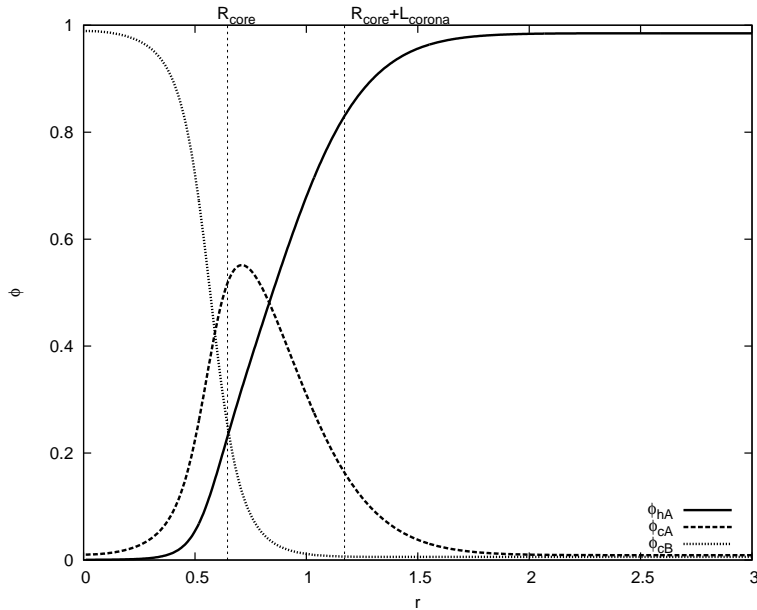


FIG. 2: Density profiles for an isolate cylindrical micelle. The blend has the parameters $f_A = 0.60$, $\kappa = 1.0$, $\chi N = 20$ and $\mu_c = 3.87$.

One of the advantages of the self-consistent field method is that detailed density profiles can be obtained for an isolated micelle. Fig. 2 shows the density profiles for the same blend examined in Fig. 1 with $\mu_c = 3.87$. With this knowledge, we are able to compute the physical properties of the micelle, such as the core radius and the corona thickness, and the material properties of the micelle, such as the number of copolymer/homopolymer

within the micelle. For the core radius, a simple definition would be using the point where $\phi_{cA}(r) = \phi_{cB}(r)$. However, this definition breaks down in the weak segregation region when sufficient amount of homopolymers are present inside the core. We opt to first calculate the radius of gyration of the core [29, 30]. For spherical micelles, the radius of gyration is defined by

$$R_{g,\text{core}}^2 = \frac{\int r^2(\phi_{cB}(r) - \phi_{cB}^b)dV}{\int(\phi_{cB}(r) - \phi_{cB}^b)dV}, \quad (11)$$

where ϕ_{cB}^b is the B-block concentration of the copolymers in the bulk phase which has to be removed to isolate the core. The core radius then can be computed from $R_{g,\text{core}}$,

$$R_{g,\text{core}}^2 = \frac{3}{5}R_{\text{core}}^2. \quad (12)$$

Following a similar procedure, we can compute the radius of gyration of the corona,

$$R_{g,\text{corona}}^2 = \frac{\int r^2(\phi_{cA}(r) - \phi_{cA}^b)dV}{\int(\phi_{cA}(r) - \phi_{cA}^b)dV}, \quad (13)$$

where ϕ_{cA}^b is the A-block concentration of copolymers in bulk. The corona thickness is related to $R_{g,\text{corona}}$ by

$$R_{g,\text{corona}}^2 = \frac{3(R_{\text{core}} + L_{\text{corona}})^5 - R_{\text{core}}^5}{5(R_{\text{core}} + L_{\text{corona}})^3 - R_{\text{core}}^3}. \quad (14)$$

For lamellar and cylindrical micelles, similar formulas can be obtained.

In order to better understand the material distribution inside the micelle, we define two more variables characterizing a micelle. The first one is the excess copolymers, defined as

$$\Omega = \frac{1}{V_{\text{micelle}}} \int_0^{R_{\text{micelle}}} (\phi_c(r) - \phi_c^b)dV, \quad (15)$$

where $R_{\text{micelle}} = R_{\text{core}} + L_{\text{corona}}$ and ϕ_c^b is the copolymer concentration in bulk. This variable characterizes the number of copolymers that are segregated. The second one is the penetrating homopolymer which has a form

$$\Theta = \frac{1}{V_{\text{micelle}}} \int_0^{R_{\text{micelle}}} \phi_{hA}(r)dV. \quad (16)$$

This variable describes the number of homopolymers which penetrate inside the micelles, which is a good indication for the degree of swelling.

III. RESULTS AND DISCUSSIONS

In general, the critical micelle concentration for a particular morphology is a function of the diblock asymmetry f_A , the homopolymer/copolymer length ratio κ , and the interaction

parameter χN . The CMC of different morphologies can be obtained from the self-consistent field theory, and the preferred micelle geometry is the one with the lowest CMC. Since the chemical potential is a monotonic function of the copolymer concentration in the dilution solution, the shape transition sequence can be obtained by comparing the copolymer chemical potential.

We begin by examining the dependence of CMC on f_A , while keeping κ and χN constant. Before we present our results, it is instructive to reproduce the results from the scaling theory [7], which can be compared with the SCFT results. In Fig. 3, the value of $\mu_{cmc}/(\chi N)^{1/3}$ for different micelle shapes are plotted as functions of the copolymer asymmetry f_A . The scaling theory predicts that the micelle geometry is lamellar for $f_A < 0.65$, cylindrical for $0.65 < f_A < 0.87$, and spherical for $f_A > 0.87$. Also, the value of f_A at which the shape transition occurs does not depend on χN , due to the coincidence that μ_{cmc} for different geometries have the same factor $(\chi N)^{1/3}$.

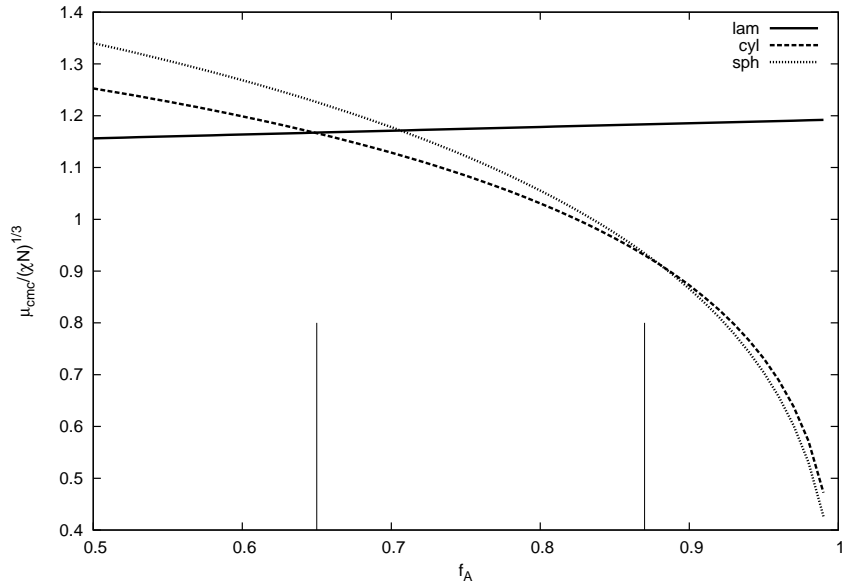


FIG. 3: Dependence of μ_{cmc} on the copolymer asymmetry f_A as derived from the scaling method. Three morphologies are plotted: lamellar (dotted line), cylindrical (dashed line) and spherical (solid line).

In the inset of Fig. 4, the critical micelle concentrations, computed from the SCFT, are plotted as a function of f_A for blends with $\kappa = 1.0$ and $\chi N = 20$. The curves for different micelle shapes are difficult to distinguish due to the small difference among them,

but the trend that the CMC is a monotonically increasing function of f_A can be seen. When f_A is increased while the total length of the copolymer kept constant, the length of B-block is reduced, which effectively reduces the incompatibility between copolymers and homopolymers. At the same time, the length of the A-block is increased, which improves the solubility of the copolymers in the homopolymers. Thus, a higher copolymer concentration is required for the formation of micelles.

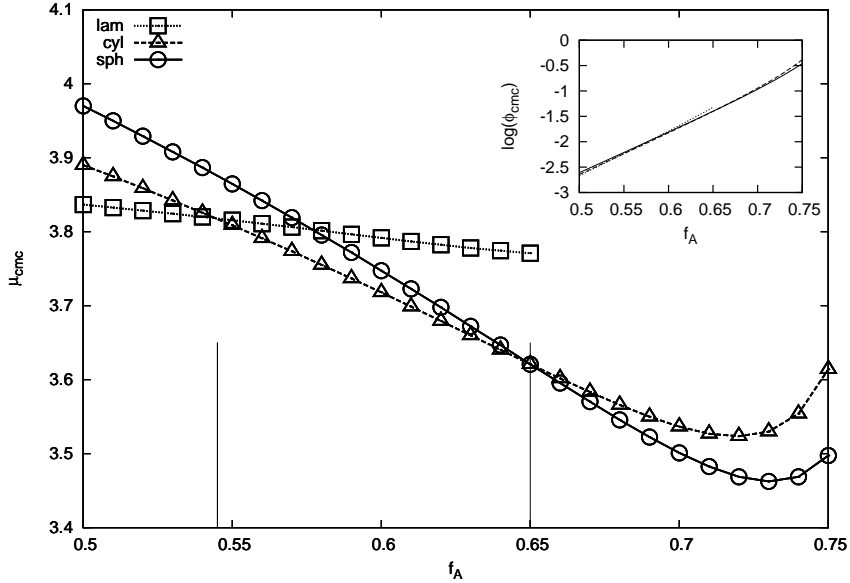


FIG. 4: Dependence of μ_{cmc} on the copolymer asymmetry f_A for blends with $\chi N = 20$ and $\kappa = 1.0$. The critical micelle concentrations are plotted in the inset. Three morphologies are plotted: lamellar (dotted line, squares), cylindrical (dashed line, triangles) and spherical (solid line, spheres).

The shape transition can be more clearly shown when we examine the chemical potential plot (Fig. 4). The chemical potential μ_{cmc} corresponding to CMC is a decreasing function of f_A for cylindrical and spherical micelles when the asymmetry is moderate, but starts to increase when the asymmetry becomes larger. In contrast to the scaling theory, the μ_{cmc} for the lamellar micelles also has a small negative slope. For copolymers with f_A close to 0.5, the chemical potential is much lower for the lamellar micelles than for the cylindrical and spherical micelles, indicating that the lamellar structure is favored. As f_A increases, μ_{cmc} decreases. The slopes are different for different geometries; the curve for spherical micelles decreases most rapidly, and the lamellar micelles have a more flat curve. The comparison

between μ_{cmc} indicates a trend of shape transition: lamellar \rightarrow cylindrical \rightarrow spherical, as f_A is increased from 0.5. This tendency can be explained by a simple geometrical argument: as f_A increases, the ratio between the volume of the corona (A-block) and core (B-block) becomes larger, causing the interfaces between A and B blocks to curve more towards the core. This transition sequence resembles that of neat diblock copolymer phases from lamellae to cylinders to spheres. For $\kappa = 1.0$ and $\chi N_c = 20$, the micelle shape transitions happen at $f_A = 0.54$ and $f_A = 0.65$.

In Fig. 5, plots similar to those in Fig. 4 are shown, only the length ratio of homopolymer/copolymer is changed to $\kappa = 2.0$. The transition points move towards copolymers with large f_A , at $f_A = 0.59$ and $f_A = 0.70$.

In Fig. 6, we increase the incompatibility between the A/B monomers to $\chi N = 50$, while keeping the homopolymer length the same. The change of χN has a pronounced effect on CMC (notice the difference in y -scale of Fig. 4 and 6 insets). Similar to Fig. 5, the transition points also shift to more asymmetric copolymers. This is in contrast to the scaling result, which states that the shape transition is independent of χN .

The shape transition of the micelle can also be induced by varying the homopolymer molecular weight. We choose to study the blends with $f_A = 0.70$ and $\chi N = 20$. For such an asymmetric diblock copolymer, the lamellar structure is unstable, so only cylindrical and spherical micelles are considered. In Fig. 7, the critical micelle concentrations are plotted as functions of κ . Since the difference in CMC between different homopolymer lengths is considerably larger than those between different shapes for a given homopolymer length, we also plot the difference of CMC in the inset to demonstrate the transition point more clearly. The micelle undergoes a sphere to cylinder transition at around $\kappa = 2.0$.

To better understand the mechanism of the shape transition, we examine the micelle core radius, the corona thickness, the excess copolymers and the penetrating homopolymers in the micelle. In Fig. 8(a), the core radius consisted mostly of the B-blocks are shown as a function of κ . The configuration of copolymer chains in the core is notably different for the two geometries. In the core of the cylindrical micelles, the B-chains are only slightly extended from their Gaussian configuration (the unperturbed rms end-to-end distance for the B-block with $f_B = 0.3$ is $0.22\sqrt{Na}$). When the homopolymer length is increased, the B chains are stretched further, but in a more gradual manner. This is because more copolymers are segregated into the micelle, as shown in Fig. 8(c). This effect counters the increase of

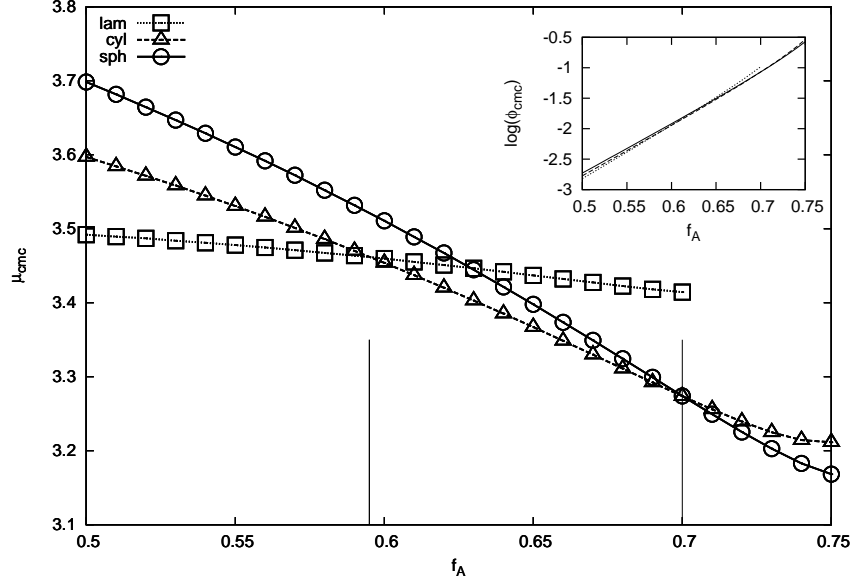


FIG. 5: Dependence of μ_{cmc} and ϕ_{cmc} on the copolymer asymmetry f_A for blends with $\chi N = 20$ and $\kappa = 2.0$. Notation as in Fig. 4.

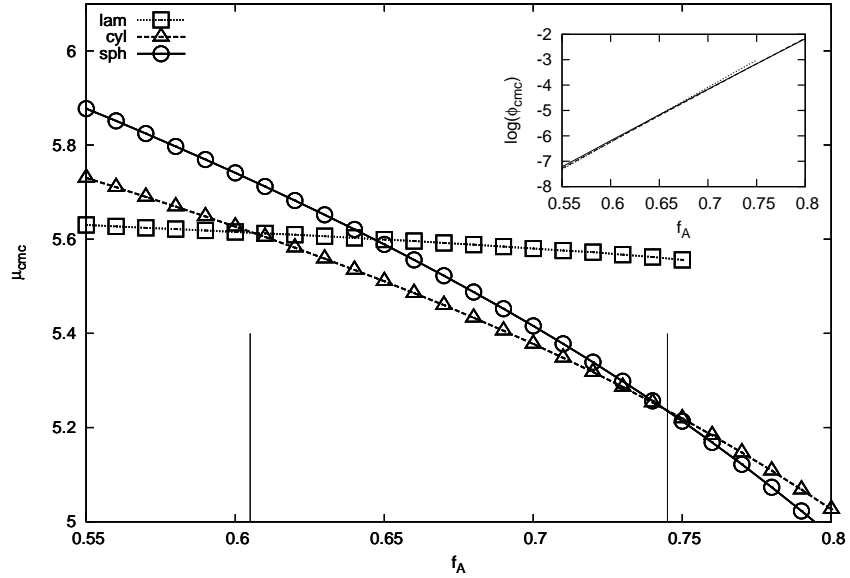


FIG. 6: Dependence of μ_{cmc} and ϕ_{cmc} on the copolymer asymmetry f_A for blends with $\chi N = 50$ and $\kappa = 1.0$. Notation as in Fig. 4.

core radius and provides some release for the B chains. For the spherical micelle, similar trends of the core radius and excess copolymers are found, but comparing to the cylindrical micelles, the B-blocks are more elongated in the spherical micelle.

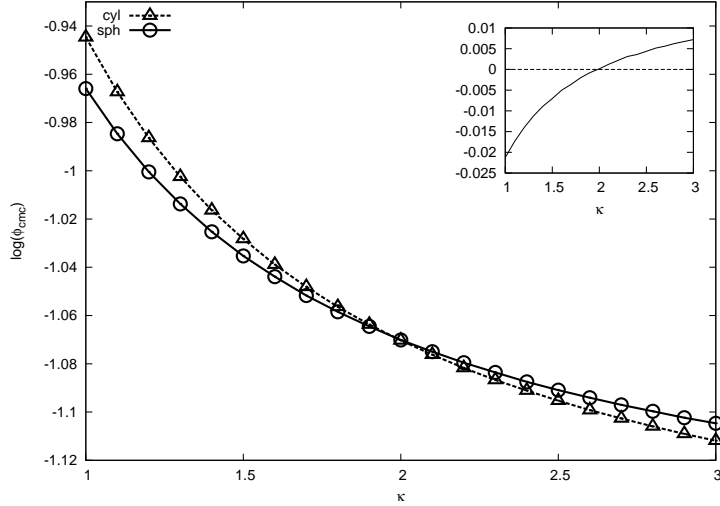


FIG. 7: Dependence of ϕ_{cmc} on the homopolymer/copolymer length ratio κ for blends with $\chi N = 20$ and $f_A = 0.70$. Two morphologies are plotted: cylindrical (dashed line, triangles) and spherical (solid line, spheres). The difference in the cmc of the two morphologies is plotted in the inset for clarity.

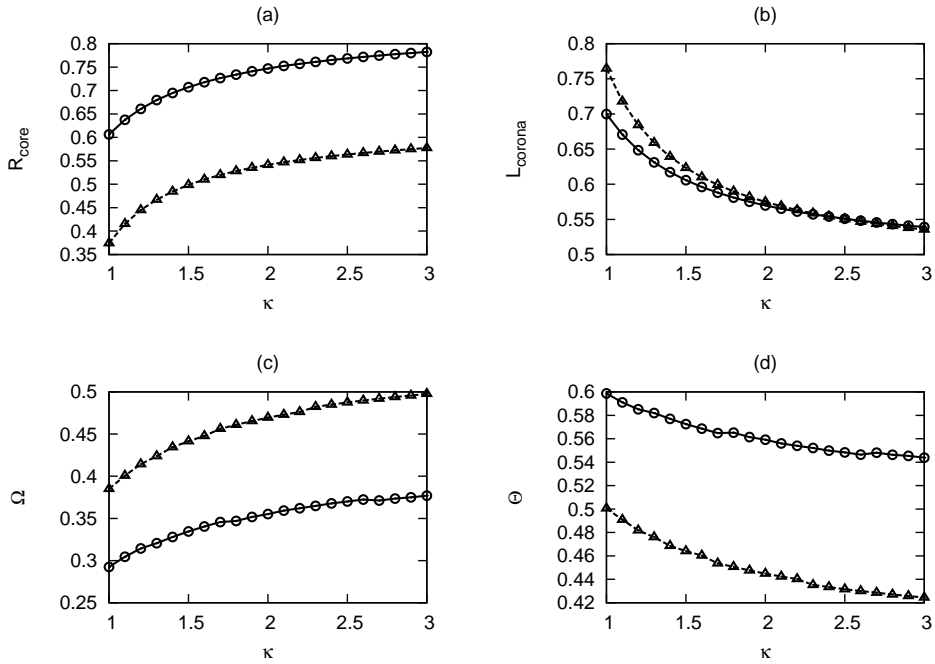


FIG. 8: Micelle properties as a function of κ for blends with $\chi N = 20$ and $f_A = 0.70$. The core radius (a), the corona thickness (b), the excess copolymers (c) and the penetrating homopolymers (d) are plotted. Notation as in Fig. 7.

The corona of the micelle consists of mostly A-blocks of the copolymer, swollen by the A-homopolymers. The corona thickness (Fig. 8(b)) appears to be much larger than the length of the unperturbed A-block ($0.34\sqrt{N}a$), indicating that the A-blocks are strongly stretched. This chain conformation is energetically unfavorable, but it can be compensated by the gain in entropy due to the mixing of A-blocks and A-homopolymers. The difference between the two morphologies lies in the degree of swelling, as shown in Fig. 8(d). The spherical micelle has more homopolymers penetrating into the corona than the cylindrical micelle. Those homopolymers help to relax the stretching of the A-blocks in the corona. When κ is increased, the size of the homopolymers becomes bigger comparing to the micelle, and it is more difficult for the homopolymers to penetrate inside the corona. Therefore, both the corona length and the swelling decreases as κ increases.

The polymer chains in both the core and the corona are strongly stretched for the two geometries. On the other hand, the formation of micelles separates the A and B monomers to avoid the unfavorable interactions. Also, the A-homopolymers can penetrate the corona to release some tension of the A-blocks. Comparing to the cylindrical micelle, there are more A-homopolymers in the corona of the spherical micelle. Thus the reduction of swelling due to increasing homopolymer length has a more profound effect on the spherical micelle, causing the shape transition from spherical micelle to cylindrical micelle, as shown in Fig. 7.

Change in the micelle morphology can also be induced by varying the interaction parameter χN . We consider blends with parameters $f_A = 0.7$ and $\kappa = 1.0$. The critical micelle concentrations and micelle properties are plotted in Fig. 9 and 10. A change of morphology from spherical to cylindrical micelle is induced when the χN is increased, similar to the case when κ is increased. However, there are some notable differences. First, the CMC changes more rapidly with varying χN . The value of the CMC is reduced by two orders of magnitude when χN changes from 20 to 40, while the CMC has the same order when κ changes from 1 to 2. Varying the homopolymer length is to change the surrounding of the micelle, while changing the interaction parameter directly alters the incompatibility between the A/B blocks of the copolymers, so the latter has a much profound effect on the CMC. Second, as shown in Fig. 10(b), there appears to be a minimum in the corona thickness when χN is increased. At the weak segregation region when χN is small, the corona is strongly swollen by the A homopolymers. As χN increases, the repulsion between the A

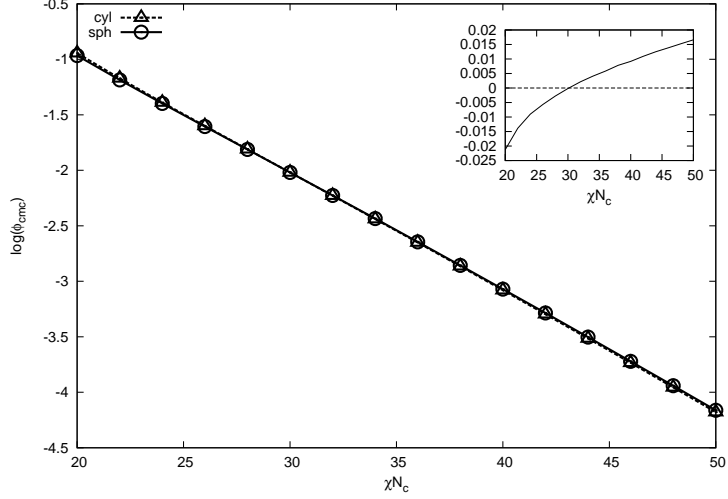


FIG. 9: Dependence of ϕ_{cmc} on the interaction parameter χN for blends with $\kappa = 1.0$ and $f_A = 0.70$. The difference in the cmc of the two morphologies is plotted in the inset for clarity. Notation as in Fig. 7

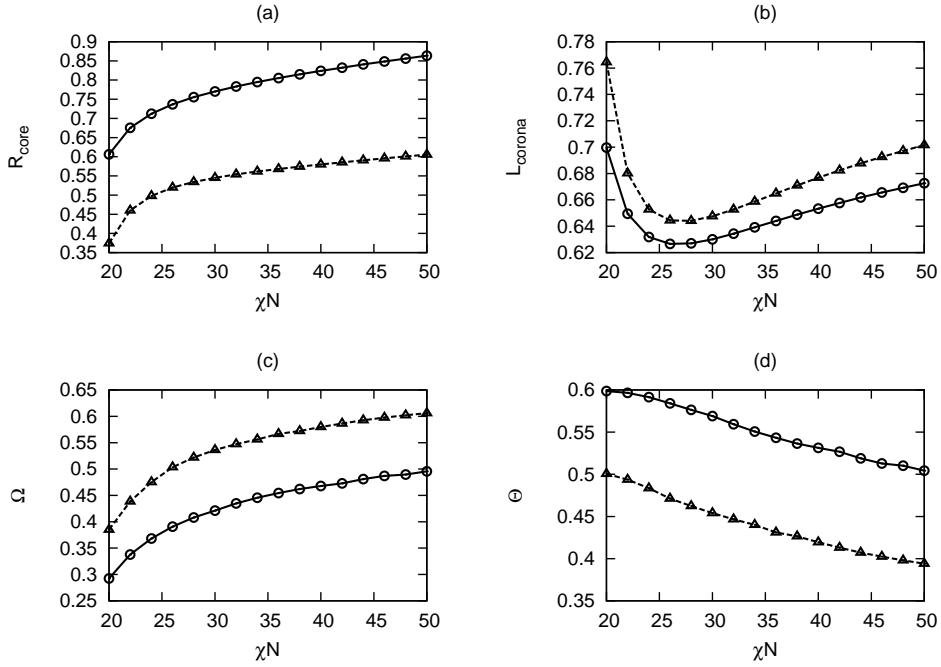


FIG. 10: Micelle properties as a function of χN for blends with $\kappa = 1.0$ and $f_A = 0.70$. The core radius (a), the corona thickness (b), the excess copolymers (c) and the penetrating homopolymers (d) are plotted. Notation as in Fig. 7.

and B monomers pushes the A homopolymers away from the corona, subsequently reducing the corona thickness. As χN becomes larger and reaches the strong segregation region, the interfacial energy becomes important. Both the A and B blocks of the copolymers have to be stretched in order to reduce the surface per copolymer; thus the corona thickness starts to increase. This is similar to the case of diblock melts, where the period of the order structure increases as χN increase.

IV. SUMMARY

In this paper, we have investigated the shape transition of an isolated micelle formed in the AB-diblock copolymer and A-homopolymer blends. Self-consistent field theory has been employed to compute the critical micelle concentration for three different morphologies: lamellar, cylindrical and spherical. By comparing the CMC for different shapes, we can determine the preferred micelle geometry. Several factors can influence the micelle morphology, and we have explored the effects of the diblock asymmetry, the homopolymer/copolymer length ratio and the monomer-monomer interaction, on the micelle shape transitions. It is found the micelle undergoes a sequence of shape transitions, lamellar \rightarrow cylindrical \rightarrow spherical, when the A-block of the copolymer becomes longer. Previous studies have showed the same transition sequence but for different ranges of homopolymer molecular weight. Mayers *et al.* [12] used the scaling argument and considered the case of $\kappa < 1$, while Termonia [22] carried out Monte Carlo simulation for the system of AB diblock copolymer in a B-selective solvent. Both studies were focused on the cylindrical and spherical micelles. Combined with results showed in Fig. 4 ($\kappa = 1$) and Fig. 5 ($\kappa = 2$), we can conclude that the transition from cylindrical to spherical micelle is a generic feature upon increasing the A-block length. In experiments, micelles with non-spherical structure were observed using transmission electron microscopy by Kinning *et al.* [4] in dilute poly(styrene-butadiene)/polystyrene solutions. They found the transition from spherical micelles to wormlike micelles by increasing the molecular weight of the butadiene block (decreasing f_A), which is in agreement with our conclusion.

For asymmetric copolymers with a large A-block, the transition from spherical to cylindrical micelle is expected when the homopolymer length is increased. The mechanism of the shape transition can be understood by examining the chain deformation inside the micelle.

As the length ratio of homopolymer/copolymer increases, the micelle core and corona exhibit the opposite variation: (i) The corona is less swollen by the longer homopolymer, leading to the relaxation of the A-blocks in the corona, and thus a smaller corona thickness. (ii) The number of copolymer chains per micelle increases due to the reduced compatibility, and thus the core radius increases. For a fixed copolymer asymmetry, the increase of core/corona ratio induces a shape transition from spherical to cylindrical micelles. The structure variations of micelles are in agreement with another experiment performed by Kinning *et al.* [37] using small angle x-ray scattering.

The same transition from sphere to cylinder appears when the repulsive interaction between different monomers becomes stronger. Similar to the case of changing κ , the core radius and number of copolymer chains per micelle increase, while the degree of swelling is reduced as χN becomes larger. These trends were observed in the experiment by Rigby and Roe [38]. They studied the micelle formation in dilute poly(butadiene-styrene)/polybutadiene solutions using small angle x-ray scattering and focused on the effect of temperature. Their observation of volume fraction of B-blocks in the core and the number of copolymer aggregating in the micelle are in agreement with the trends shown in Fig. 10 (d) and (c), but the core radius is insensitive to the temperature in certain ranges and increases suddenly at high temperature. This may attribute to the fairly small molecular weight of homopolymer used in the experiments. When κ is small, the micelles are highly swollen by the homopolymer, and our definition of core radius may not correspond to that measured in experiments.

Our self-consistent field calculations demonstrate that valuable information can be obtained, such as the geometrical dimensions of the micelle, and the distribution of the polymers inside the micelle. These properties are closely related to the controlling parameters. By varying these parameters, micelle with required shape and size may be obtained for potential applications. Since it is expensive and time-consuming for experimentalists to explore the parameter space by trial-and-error, theoretical study is crucially important to understand the underlying cause and provide guidance for the experiments.

It is important to point out the limitation of the present approach. Since we have neglected the translational entropy of the micelles, the critical micelle concentrations calculated are qualitatively correct. Also, for lamellar and cylindrical micelles, we only considered the ideal case, while in reality, infinite long cylinders and infinite broad bilayers can not be

formed. The ends of the cylinders or the edges of the lamellae will have a contribution to the free energy, so the points of shape transition needed be modified accordingly. Furthermore, cylindrical micelles can form loops while lamellar micelles can form vesicles. Investigation these more complex micellar structures is an important topic. Nevertheless, by comparing the minimum copolymer concentration required for micellization in three geometries under ideal conditions, we have obtained the trends in dilute systems of diblock copolymer with homopolymers. The results obtained in the current study are consistent with available theoretical and experimental studies. They provide a detailed picture of the micelles with different shapes and a good understanding of the mechanism of micelle shape transitions.

Acknowledgments

This work was supported by the Natural Sciences and Engineering Research Council (NSERC) of Canada. The computation was made possible by the facilities of the Shared Hierarchical Academic Research Computing Network (SHARCNET:www.sharcnet.ca) and Compute/Calcul Canada.

-
- [1] Hamley, I. *The Physics of Block Copolymers*; Oxford University Press: Oxford, 1998.
 - [2] Riess, G. *Prog. Polym. Sci.* **2003**, *28*, 1107–1170.
 - [3] Safran, S. A. *Statistical Thermodynamics of Surfaces, Interfaces, and Membranes*; Addison-Wesley: New York, 1994.
 - [4] Kinning, D. J.; Winey, K. I.; Thomas, E. L. *Macromolecules* **1988**, *21*, 3502.
 - [5] Kim, Y.; Dalhaimer, P.; Christian, D.; Discher, D. *Nanotechnology* **2005**, *16*, S484.
 - [6] Leibler, L. *Makromol. Chem., Macromol. Symp.* **1988**, *16*, 1.
 - [7] Shull, K. R.; Kramer, E. J.; Hadziioannou, G.; Tang, W. *Macromolecules* **1990**, *23*, 4780.
 - [8] Shull, K. R. *Macromolecules* **1993**, *26*, 2346.
 - [9] Leibler, L.; Orland, H.; Wheeler, J. C. *J. Chem. Phys.* **1983**, *79*, 3550.
 - [10] Whitmore, M. D.; Noolandi, J. *Macromolecules* **1985**, *18*, 657–665.
 - [11] Roe, R. J. *Macromolecules* **1986**, *19*, 728–731.
 - [12] Mayes, A. M.; de la Cruz, M. O. *Macromolecules* **1988**, *21*, 2543.

- [13] Kao, C. R.; de la Cruz, M. O. *J. Chem. Phys.* **1990**, *93*, 8284.
- [14] Milchev, A.; Bhattacharya, A.; Binder, K. *Macromolecules* **2001**, *34*, 1881–1893.
- [15] Mackie, A. D.; Panagiotopoulos, A. Z.; Szleifer, I. *Langmuir* **1997**, *13*, 5022–5031.
- [16] Guerin, C. B. E.; Szleifer, I. *Langmuir* **1999**, *15*, 7901–7911.
- [17] Smit, B.; Esselink, K.; Hilbers, P. A. J.; Van Os, N. M.; Rupert, L. A. M.; Szleifer, I. *Langmuir* **1993**, *9*, 9–11.
- [18] Wijmans, C. M.; Linse, P. *Langmuir* **1995**, *11*, 3748–3756.
- [19] Pepin, M. P.; Whitmore, M. D. *Macromolecules* **2000**, *33*, 8644–8653.
- [20] Pepin, M. P.; Whitmore, M. D. *Macromolecules* **2000**, *33*, 8654–8662.
- [21] Kenward, M.; Whitmore, M. D. *J. Chem. Phys.* **2002**, *116*, 3455–3470.
- [22] Termonia, Y. *J. Polym. Sci. Part B: Polym. Phys.* **2002**, *40*, 890–895.
- [23] Cavallo, A.; Müller, M.; Binder, K. *Macromolecules* **2006**, *39*, 9539–9550.
- [24] Sheng, Y.-J.; Wang, T.-Y.; Chen, W. M.; Tsao, H.-K. *J. Phys. Chem. B* **2007**, *111*, 10938–10945.
- [25] Linse, P. *Macromolecules* **1993**, *26*, 4437.
- [26] Leermakers, F.; Wijmans, C.; Fleer, G. *Macromolecules* **1995**, *28*, 3434.
- [27] Duque, D. *J. Chem. Phys.* **2003**, *119*, 5701–5704.
- [28] Chang, K.; Morse, D. C. *Macromolecules* **2006**, *39*, 7746–7756.
- [29] Greenall, M. J.; Buzza, D. M. A.; McLeish, T. C. B. *Macromolecules* **2009**, *42*, 5873.
- [30] Greenall, M. J.; Buzza, D. M. A.; McLeish, T. C. B. *J. Chem. Phys.* **2009**, *131*, 034904.
- [31] Schmid, F. *J. Phys.: Condens. Matter* **1998**, *10*, 8105.
- [32] Fredrickson, G. H.; Ganesan, V.; Drolet, F. *Macromolecules* **2002**, *35*, 16.
- [33] Matsen, M. *J. Phys.: Condens. Matter* **2002**, *14*, R21.
- [34] Shi, A.-C. In *Developments in Block Copolymer Science and Technology*; Hamley, I., Ed.; John Wiley & Sons: New York, 2004; Chapter 8.
- [35] Fredrickson, G. H. *The Equilibrium Theory of Inhomogeneous Polymers*; Clarendon Press: Oxford, 2006.
- [36] Press, W. H.; Teukolsky, S. A.; Vetterling, W. T.; Flannery, B. P. *Numerical Recipes*, 3rd ed.; Cambridge University Press: New York, 2007.
- [37] Kinning, D. J.; Thomas, E. L.; Fetters, L. J. *J. Chem. Phys.* **1989**, *90*, 5806–5825.
- [38] Rigby, D.; Roe, R. J. *Macromolecules* **1984**, *17*, 1778–1785.